

# Angular Momentum of Photon and Phase Conjugation.

**A.Yu.Okulov**

General Physics Institute  
of Russian Academy of Sciences  
Vavilova str. 38, 119991, Moscow, Russia

E-mail: okulov@kapella.gpi.ru

## Abstract.

Using concept of an *ideal* phase-conjugating mirror we demonstrate that regardless to internal physical mechanism the phase-conjugation of singular laser beam is accompanied by excitation within mirror of internal waves which carry doubled angular momentum in order to match angular momentum conservation. For Brillouin hypersound wavefront-reversal mirror this means that each elementary optical vortex in a speckle pattern emits acoustical vortex wave with doubled topological charge. The exact spatial profiles of light intensity and intensity of hypersound in the vicinity of phase singularity are obtained. These *spiral* profiles have a form of a double helix which rotates with the speed of sound. The optoacoustic experiment is proposed for visualization of wavefront reversal of twisted optical beams and tunable twisted sound generation.

The conservation of angular momentum (**AM**)  $\vec{J}$  stems from isotropy of space [1]. In contrast to particles with nonzero rest mass  $m_o$ , the decomposition of  $\vec{J}$  for "spin"  $\vec{S}$  and "orbital"  $\vec{L}$  parts of photon's **AM** is referred to as ambiguous procedure [1, 2]. The spin part  $\vec{S}$  is related to polarization, i.e. time-dependent layout of electrical  $\vec{E}$  and magnetic  $\vec{B}$  fields of the "transverse" light wave. The orbital part (**OAM**)  $\vec{L}$  is associated with helical staircase wavefront [2, 3, 4, 5]. As a matter of fact a purely transverse light waves are abstraction because of a small but inevitable projections of  $\vec{E}$  and  $\vec{B}$  on direction of propagation, say  $Z$ -axis(fig.1). Indeed, the spin-orbital coupling of light occurs [6] due to vectorial interplay between longitudinal and transversal components of the fields  $\vec{E}$  and  $\vec{B}$ . The vectorial solutions of Maxwell's equations for propagation of a light spatially localized by a waveguide or emitted through finite aperture to free space give a strict relationship between longitudinal and transversal field components [7, 8]. Nevertheless the approximate decomposition in the form  $\vec{J} = \vec{S} + \vec{L}$  proved to be very fruitful for small curvatures of light wavefront, i.e. in paraxial wave approximation[2].

The propagation of light in anisotropic medium changes the polarization and historically the spin of photon was observed firstly in Beth's experiment where

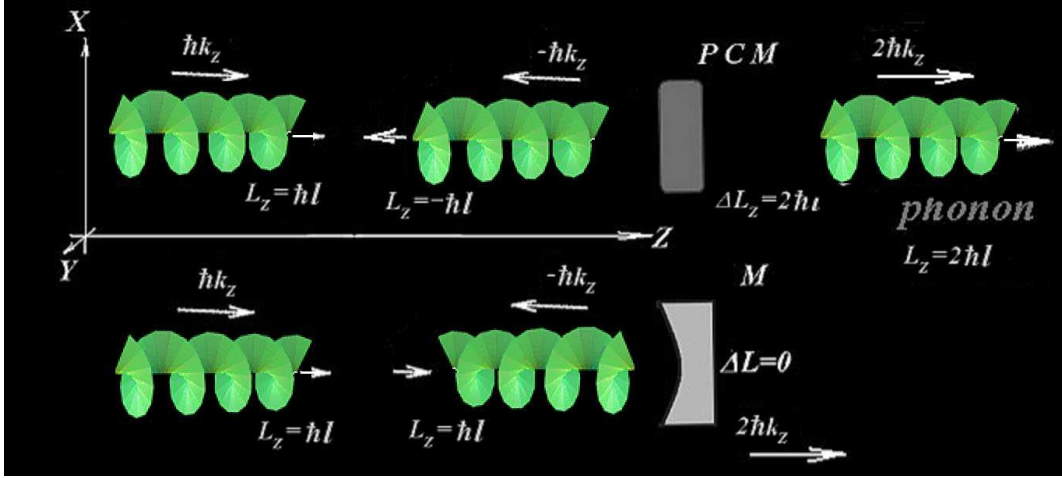


**Figure 1.** Comparison of conventional mirror (**M**,bottom) and wavefront reversal mirror (**PCM**,upper) from the point of view of angular momentum transformation in photon's reflection. Upper view: The "right" photon with plane polarization and helical wavefront strikes **PCM** and decays to "right" photon, moving to opposite direction with momentum  $-\hbar k_z$ . The acoustical phonon absorbs *translational recoil* momentum  $2\hbar k_z$  and *rotational recoil OAM*  $2\hbar$ . Bottom view: The "right" photon with topological charge +1 strikes the conventional mirror **M** and transforms to "left" photon. In this case the **OAM** is not changed and *rotational recoil* is absent.

birefringent  $\lambda/2$  plate induced the change of photon polarization from circular ( $S_z = +\hbar$ ) to counter-rotating one ( $S_z = -\hbar$ ) [9]. The elementary act of photon's spin change accompanied by back action and stepwise increase of angular momentum of a plate. The quantum-classical correspondence fulfilled by origin of a macroscopically observable classical torque  $\vec{T} = \frac{d}{dt} \vec{J} = [\vec{D} \times \vec{E}]$  [2], where  $|\vec{J}| \approx \frac{I}{\omega}$ ,  $\omega$  - is angular frequency and  $I$  - is intensity of light.

The reflection of circularly polarized photon from an ideal conventional mirror (metal or multilayer dielectric one) does not change the direction of both spin  $\vec{S}$  and orbital momentum  $\vec{L}$  in the laboratory frame and mechanical torque  $\vec{T}$  on such mirror is absent (fig.1). This follows both from boundary conditions for Maxwell equations[8] and from rotational symmetry of setup with respect to  $Z$ -axis[1, 10].

The current communication pays particular attention to conservation laws in reflection of photon carrying **OAM**  $L_z = \ell\hbar$  from *phase-conjugating mirror (PCM)*. The discussion will be concentrated mainly upon Brillouin wavefront-reversal mirror [10]. We will demonstrate the hidden anisotropy of SBS-mirror which arise due to excitation of internal helical waves, i.e. acoustical vortices, whose existence had been proven recently for *Mhz*-range sound [11]. The rotation of ultracold cesium atoms [12] also had been suggested to occur because of **OAM** transfer due to backward reflection of Laguerre-Gaussian beam (**LG**) with 0.001 diffractive efficiency via nondegenerate four-wave mixing process. The **OAM** transfer from co-propagating circularly **LG** to BEC [13] had been discussed as well.

The circularly polarized photon is called "right" when projection of the spin  $S_z$

upon direction of propagation is positive(fig.1). This happens for example, when photon moves in positive direction of  $Z$ -axis with momentum  $\hbar\vec{k}$  and the fields  $\vec{E}$  and  $\vec{B}$  rotate clockwise with respect to  $\vec{k}$ . On the contrary the "left" photon have counter-clockwise rotation of polarization and it carries spin  $S_z = -\hbar$ .

In reflection from conventional mirror the incident "right" photon with  $S_z = +\hbar$  moving in positive direction of  $Z$ -axis with momentum  $p_z \approx \hbar|\vec{k}|$  is transformed in a "left" photon having  $p_z \approx -\hbar|\vec{k}|$  and the *same* spin projection  $S_z = +\hbar$ . And vice versa, when incident "left"(or counter-clockwise) photon strikes mirror, the sign of  $S_z = -\hbar$  is not changed in laboratory frame and photon becomes "right". It is not surprising because setup is isotropic. In this situation the only mechanical effect on mirror is light pressure [14, 15], whose major component is normal to mirror surface. So the conventional mirror in *normal* reflection accepts the momentum  $\Delta p_z \approx 2\hbar\vec{k}$  as a single entity and does not change both polarization (or spin  $\vec{S}$ ) and orbital momentum  $\vec{L}$ .

The situation is changed drastically for **PCM** [10]. The conservation laws determine the energy of excited acoustical phonon  $\hbar\Omega_a$  as a difference of energies of incident  $\hbar\omega_p$  and reflected  $\hbar\omega_s$  photons. The radiation pressure also takes place here because of net momentum transfer to sound  $p_{phonon} = \Delta p_z \approx 2\hbar k_z$  or "recoil". The most interesting feature is the conservation of **OAM**  $\vec{L}$ . Let us show that the wavefront-reversal mirror should feel "rotational recoil" when vortex beam carrying **OAM** is reflected with ultimate phase conjugation fidelity. Indeed, because of the basic feature of phase-conjugation the retroreflected photon passes all states of the incident one in reverse sequence [16]. This is a so-called *time reversal* property of the wavefront-reversing mirror. Consequently the helicoidal phase surfaces of incident photon and reflected photon should be perfectly matched (fig.1). The small mismatch of the wavefronts caused by recoil frequency shift and wavenumber shift of the order  $10^{-5}$  [16] does not affect the phase surfaces. Because of accurate wavefront's match the **OAM** is turned to  $180^\circ$  angle and **OAM** projection  $L_z = +\ell\hbar$  is changed to the opposite one  $L_z = -\ell\hbar$ . As a consequence the "winding" number or topological charge  $\ell$  does not change the sign with respect to propagation direction  $\vec{k}$ . Thus the conjugated photon with "right" **OAM** remains "right", the photon with "left" **OAM** remains "left".

The apparent physical consequence of this fact is the necessity of excitation of *internal wave* which ought to absorb the difference of angular momenta  $\Delta L_z = +2\ell\hbar$  before and after retroreflection. Consequently this internal wave should have singular wavefront unavoidably provided the **PCM** is ideal. At this point let us stress again upon remarkable difference between *spin*  $\vec{S}$  and *orbital*  $\vec{L}$  components of angular momentum. The electrostrictive nonlinearity in isotropic medium is scalar in paraxial approximation at least and spin part of **AM** is not turned to opposite one[10]. On the contrary, the orbital component  $\vec{L}$  or **OAM** does turns, because acoustical vortices do exist[11]. It will be shown below in details by *exact analytical formulas* how acoustical vortices absorb the **OAM**. In fact there exist some obstacles in realization of the perfect phase-conjugation of elementary optical vortices say in the form of **LG** [17]. Nevertheless

it will be shown below how to overcome this class of difficulties using traditional and reliable methods of the Brillouin phase-conjugation[16].

For this purpose let us separate the region of wavefront reversal via traditional phase-conjugating mechanisms, e.g. Brillouin **PCM** and optoacoustic cell (**OA**) where sound is excited parametrically, without back action on light(fig.2). This geometry makes possible to visualize inside **OA** acoustical vortex collocated with the optical phase singularity in a spatial region having size up to several millimeters in transverse dimensions, i.e. in  $X, Y$ -plane[11].

The acoustical waves inside Brillouin **PCM** volume are highly dissipative, because hypersound have a typical relaxation times about  $10^{-9} \text{ sec}$ [10]. In liquid crystals, which are used for phase-conjugation the relaxation times are significantly longer -  $10^{-3} \text{ sec}$ [10]. In the second case one might expect to observe the macroscopic torque on **PCM** for appropriate time scales. Or else in anisotropic artificial medium alike Veselago's lens [18] might appear a macroscopic rotational recoil caused by optical torque.

Consider for definiteness the interaction of the two counter-propagating paraxial laser beams inside Brillouin active medium. Instead of the quantized field description by means of Heisenberg's secondary-quantization  $\hat{\Psi}$  - operators [1] we choose more intuitive approach using classical counter-propagating optical fields  $\mathbf{E}_p$ ,  $\mathbf{E}_s$  and acoustic field  $\mathbf{Q}$ . The linearly polarized "pump" field  $\mathbf{E}_p$  moves in positive direction of  $Z$ -axis, the reflected Stokes field  $\mathbf{E}_s$  with the same polarization propagates in opposite direction(fig.3). The acoustic field  $\mathbf{Q}$  is excited via electrostriction. The cylindrical system of coordinates  $(z, r, \phi, t)$  is choosed for equations below. The connection with cartesian coordinates used in figures is supposed to be evident. The "parabolic" equations of motion are well known[10]. The "envelope" complex amplitude of pump wave  $E_p$  moving from left to right (fig.1) follows to:

$$\frac{\partial E_p(z, r, \phi, t)}{\partial z} + \frac{n}{c} \frac{\partial E_p}{\partial t} + \frac{i}{2k_p} \Delta_{\perp} E_p = \frac{i\gamma\omega_p}{4\rho_0 n c} Q E_s, \quad (1)$$

The Stokes wave "envelope"  $E_s$  moving from right to left is controlled by:

$$\frac{\partial E_s(z, r, \phi, t)}{\partial z} - \frac{n}{c} \frac{\partial E_s}{\partial t} - \frac{i}{2k_s} \Delta_{\perp} E_s = -\frac{i\gamma\omega_s}{4\rho_0 n c} E_p Q^*, \quad (2)$$

The acoustic wave "envelope"  $Q$  moving from left to right obeys to:

$$v_a \frac{\partial Q(z, r, \phi, t)}{\partial z} + \frac{\partial Q}{\partial t} + \frac{\Gamma Q}{2} = \frac{i\gamma k_a^2}{16\pi\Omega_a} E_p E_s^*, \quad (3)$$

where  $\gamma = \rho(\partial\epsilon/\partial\rho)$  - is the electrostrictive coupling constant,  $\rho_0$  - is the density of medium,  $n$  - is the index of refraction,  $c$  - is the speed of light,  $v_a$  - is a speed of sound[19]. The connections between "envelope" complex amplitudes  $E_p, E_s, Q$  and complete field amplitudes  $\mathbf{E}_p, \mathbf{E}_s, \mathbf{Q}$  are given by [10, 19]:

$$\mathbf{E}_p = \exp[i(+k_p z - \omega_p t)] E_p(z, r, \phi, t);$$

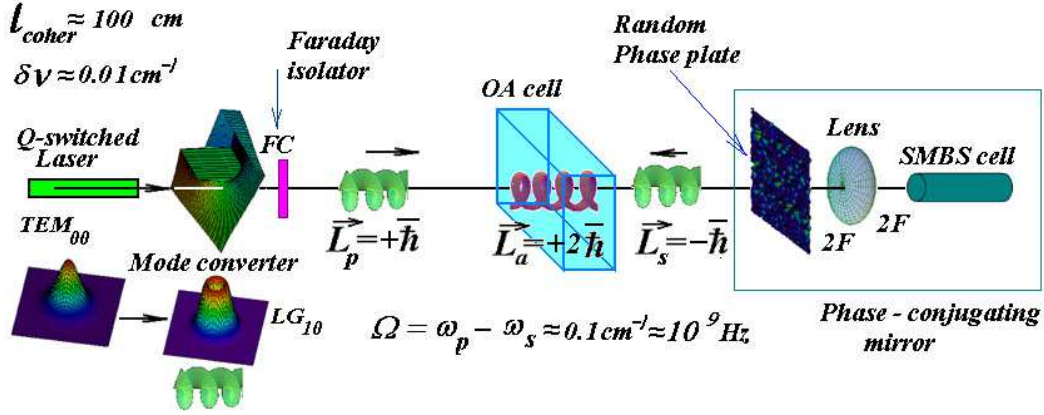


**Figure 2.** The proposal of experimental setup for twisted hypersound observation. The laser field  $E_p$  comes through mode converter and Faraday cell **FC** to optoacoustic cell **OA**. The transparent random phase plate is used for initiation of a high-fidelity phase-conjugation in multimode Brillouin-active waveguide **SBS**. **F**-is focal distance of a lens. The phase conjugated Stokes field  $E_s$  interferes with pump field  $E_p$  inside **OA** to produce rotating spiral interference pattern with transverse size of several millimeters. The *twisted sound phonons* excited by counter-propagating fields are expected to have **OAM**  $L_a = 2\hbar$  directed to right. The angular speed of rotation is equal to acoustical frequency  $\Omega_a \approx 10^9 \text{ Hz}$ .

$$\begin{aligned}
 \mathbf{E}_s &= \exp [i(-k_s z - \omega_s t)] E_s(z, r, \phi, t) \\
 \mathbf{Q} &= \exp [i(+k_a z - \Omega_a t)] Q(z, r, \phi, t)
 \end{aligned} \tag{4}$$

The equations (1-3) are valid within both Brillouin mirror and **OA** (fig.2). The solution of (1-3) for **OA** could be obtained under natural physical assumption that amplitudes  $\mathbf{E}_p$  and  $\mathbf{E}_s$  are small enough and acoustic field  $\mathbf{Q}$  is excited parametrically, by electrostrictive force in a right-hand side of (3). This assumption enables us to solve (1-2) in free-space approximation, i.e. without right-hand sides. For Cauchy propagation problem with first order Laguerre-Gaussian beam as initial condition for  $\mathbf{E}_p$  (from left window of **OA**) and  $\mathbf{E}_s$  (from right window of **OA**) we have the following *exact* solutions for pump field  $\mathbf{E}_p$  :

$$\mathbf{E}_p(z, r, \phi, t) \sim \frac{E_p^o \exp [i(+k_p z - \omega_p t) + i\ell\phi]}{(1 + iz/(k_p D^2))^2} r^\ell \exp \left[ -\frac{r^2}{D^2(1 + iz/(k_p D^2))} \right], \tag{5}$$

and for Stokes field  $\mathbf{E}_s$  :

$$\mathbf{E}_s(z, r, \phi, t) \sim \frac{E_s^o \exp [i(-k_s z - \omega_s t) + i\ell\phi]}{(1 + iz/(k_s D^2))^2} r^\ell \exp \left[ -\frac{r^2}{D^2(1 + iz/(k_s D^2))} \right]. \tag{6}$$

The fields  $\mathbf{E}_p$  and  $\mathbf{E}_s$  carry angular momentum  $\ell\hbar$  per photon[5], where  $\ell$  is above mentioned "topological charge" or "winding number",  $D$  - is diameter of beam "necklace" at full width half-maximum(FWHM),  $z$  - is distance passed along  $Z$  - axis from beam necklace,  $r = |\vec{r}|$  - length of radius vector perpendicular to  $Z$ ,  $\phi$ -azimuthal angle,  $E_s^o$  and  $E_p^o$  - are the maximal electrical field amplitudes in necklace. The maximally simplified form of the free-space solution choosed for **LG** beam [20] under

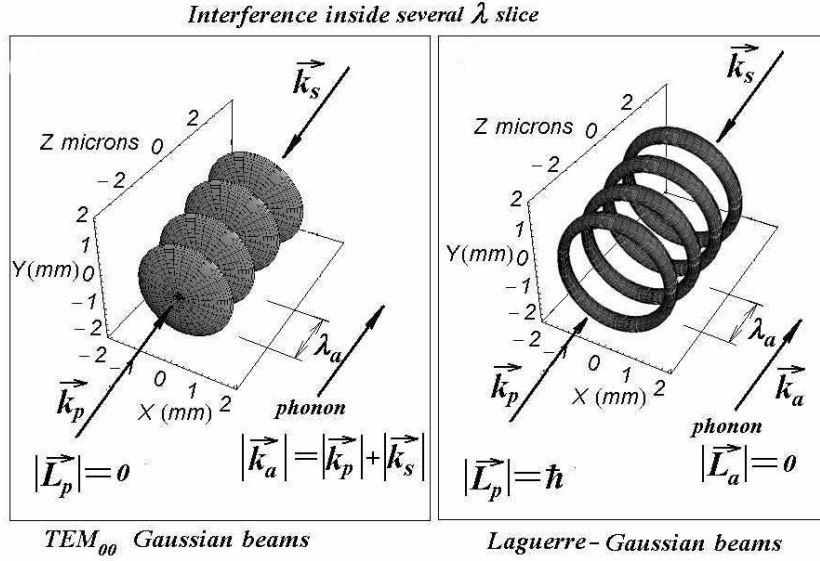


**Figure 3.** Interference pattern of incident (pump) Gaussian mode wave  $E_p$  with field  $E_s$  reflected from conventional mirror. Left : incident zeroth-order Gaussian beam forms moving quasi-sinusoidal pattern with period  $\lambda/2$  due to interference with reflected beam. Four isosurfaces of interference maxima are shown. The direction of pattern motion is changed with the change of the sign of  $\Omega$ . The pattern is the same for reflection of **TEM<sub>00</sub>** beam from **M** and **PCM**. The period of acoustical grating is equal roughly to a half of the pumping wavelength in order to satisfy Bragg reflection condition. Right: **LG** beam interferes with **LG** reflected from conventional mirror. A sequence of toroidal rings occurs. The **OAM** is not transferred to medium.

assumption that Fresnel number for *OA – cell* is large enough  $N_f = k_{p,s}D^2/z \gg 1$  or thickness of **OA** is much shorter than *Rayleigh range*  $k_{p,s}D^2$ .

Consider first the interference patterns produced by two counter-propagating fields  $\mathbf{E}_p$  and  $\mathbf{E}_s$  with equal amplitudes  $E_{p,s}^o$  and without phase singularities, i.e. two zeroth-order Gaussian beams or **TEM<sub>00</sub>** - beams near their overlapping necklaces:

$$\mathbf{E}_{(p,s)}(z, r, \phi, t) \approx E_{p,s}^o \exp \left[ -i\omega_{(p,s)}t \pm ik_{(p,s)}z - \frac{r^2}{D^2(1 \pm iz/(k_{(p,s)}D^2))} \right] \quad (7)$$

The isosurfaces of intensity  $I_{surface} < 2|E_0|^2$  as a functions of cylindrical coordinates  $(z, r, \phi, t)$  are the solutions of the following *implicit* equation reminiscent to basic course of physical optics:

$$\begin{aligned} \mathbf{I}_{isosurface} &= |\mathbf{E}(z, r, \phi, t)|^2 = |\mathbf{E}_p(z, r, \phi, t) + \mathbf{E}_s(z, r, \phi, t)|^2 \\ &\cong 2|E_{p,s}^o|^2 [1 + \cos[(\omega_p - \omega_s)t - (k_p + k_s)z]] \exp \left[ -\frac{2r^2}{D^2(1 + z^2/(k_p^2 D^4))} \right]. \quad (8) \end{aligned}$$

Apart from familiar interference term  $\cos[(\omega_p - \omega_s)t + (k_p + k_s)z]$  which describes grating with period  $\mathcal{P} = 2\pi(k_p + k_s)^{-1}$  moving along *Z – axis* with acoustical speed  $v_a = [(\omega_p - \omega_s)/(k_p + k_s)]$  the Gaussian function arose which modulates the *rolls*

of interference pattern in transverse direction. Thus the isosurfaces of intensity are pancake-like *rotational ellipsoids* separated by distance  $\mathcal{P}$  (fig. 3). Such interference pattern is in a strict agreement with the Doppler's mechanism of Brillouin scattering: the pump field is being reflected from grating which moves with the speed  $v_a$ . The resulting Doppler shift  $\omega_p - \omega_s$  is such that optical interference pattern perfectly overlaps with spatial profile of acoustic field. The left picture of (fig. 3) illustrates this moving interference pattern for four periods. In conventional picture of stimulated Brillouin scattering this moving pattern coincides with the moving profile of hypersound wave [10]. The spatial period of this wave  $\mathcal{P} = \lambda_a = 2\pi/(k_p + k_s)$  is such that Bragg condition for normal reflection from moving grating  $((\lambda_p)^{-1} + (\lambda_s)^{-1} = (\lambda_a)^{-1})$  is satisfied.

Suppose now that first order **LG** is reflected from conventional, non phase-conjugating parabolic mirror (fig. 1). Because orbital angular momentum is not changed in such reflection in *laboratory* frame, the helical terms  $(\ell\phi)$  have identical signs in expressions for fields  $\mathbf{E}_p$  and  $\mathbf{E}_s$ :

$$\mathbf{E}_{(p,s)}(z, r, \phi, t) \approx E_{p,s}^o r^\ell \exp \left[ -i\omega_{(p,s)}t \pm ik_{(p,s)}z + i\ell\phi \right] - \frac{r^2}{(D^2(1 \pm iz/(k_{(p,s)}D^2)))} \quad (9)$$

Then two counter-propagating first-order **LG** produce in **OA** more complicated interference pattern, with a *hole* on the beam axis. As a result instead of sequence of ellipsoids we have a sequence of a toroidal rings separated by period  $\lambda_a = 2\pi(k_p + k_s)^{-1}$  in order to fulfill Bragg resonant condition (fig. 3):

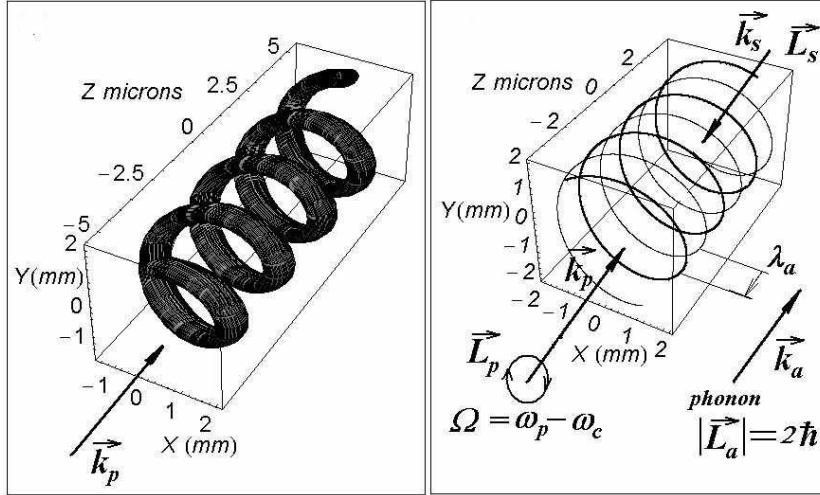
$$\mathbf{I}_{isosurface} = |\mathbf{E}(z, r, \phi, t)|^2 = |\mathbf{E}_p(z, r, \phi, t) + \mathbf{E}_s(z, r, \phi, t)|^2 \approx 2|E_{p,s}^o|^2 [1 + \cos[(\omega_p - \omega_s)t - (k_p + k_s)z]] r^\ell \exp \left[ -\frac{2r^2}{D^2(1 + z^2/(k_p^2 D^4))} \right]. \quad (10)$$

Again the interference pattern moves along  $Z$  - axis with acoustic speed  $v_a$ . The direction of motion is determined by the sign of difference  $(\omega_p - \omega_s)$ . For *anti - Stokes* difference of frequencies the interference pattern moves in negative direction of  $Z$  - axis.

Phase conjugation of **LG** changes the interference pattern drastically. Because orbital angular momentum is changed to opposite one in wavefront reversal process, the helical terms  $\ell\phi$  have *opposite signs* in expressions for fields  $\mathbf{E}_p$  and  $\mathbf{E}_s$  and expression for the Stokes field generated by **PC** - mirror reads:

$$\mathbf{E}_{(p,s)}(z, r, \phi, t) \approx E_{p,s}^o r^\ell \exp \left[ -i\omega_{(p,s)}t \pm ik_{(p,s)}z \pm i\ell\phi \right] - \frac{r^2}{(D^2(1 \pm iz/(k_{(p,s)}D^2)))} \quad (11)$$

This mathematical peculiarity, namely  $\pm$  before azimuthal angle  $\phi$ , follows from the physical fact that after retroreflection the ideally phase-conjugated wave passes all states of incident wave in reverse sequence ([16]). As a result the expression for interference pattern is slightly different:



*Phase-conjugated Laguerre-Gaussian beams*

**Figure 4.** Interference pattern of incident "right" (pump) first order **LG** wave  $E_p$  and phase-conjugated "right" replica  $E_s$ . The topological charge is  $\ell = +1$ . Left: The spiral distribution of intensity occurs. The only one string is shown because of computational power limitations. Right: Actually the interference pattern have the form of a *double helix*. The right plot depicts the maxima of intensity only. The double helix rotates clockwise when the frequency difference is positive (Stokes case). For anti-Stokes retroreflection the rotation of helix is counter-clockwise. The period of acoustical spring is equal roughly to a half of the pumping wavelength for Brillouin scattering.

$$\begin{aligned} \mathbf{I}_{isosurface} &= |\mathbf{E}(z, r, \phi, t)|^2 = |\mathbf{E}_p(z, r, \phi, t) + \mathbf{E}_s(z, r, \phi, t)|^2 \approx \\ &2|E_{s,p}^o|^2 [1 + \cos[(\omega_p - \omega_s)t - (k_p + k_s)z + 2l_w \phi]] r^{2l_w} \\ &\exp \left[ -\frac{2r^2}{D^2(1 + z^2/(k_p^2 D^4))} \right]. \end{aligned} \quad (12)$$

The self-similar variable  $(\omega_p - \omega_s)t - (k_p + k_s)z$  in the argument of  $\cos$  acquires the *doubled azimuthal angle*  $2l\phi$ . As a consequence the interference pattern changes from sequence of toroidal rings to double helix (fig. 4). The spiral interference pattern has *two maxima* because azimuthal dependence contains *doubled* azimuthal angle  $\phi$ . The spatial period of the springs is again automatically adjusted in such a way that one may say *generalized* Bragg condition is satisfied. The other drastical feature is that interference pattern *rotates* with angular velocity equal to *acoustical frequency*  $\Omega_a = (\omega_p - \omega_s)$ . The linear, translational speed of  $Z$ -aligned motion of a helix's turns is exactly equal to the sonic speed  $v_a$ :

$$v_a = \frac{(\omega_p - \omega_s)}{(k_p + k_s)} \quad (13)$$

The similar double-helix structures were reported recently for a Wigner crystals in a dusty plasma [21].



The singular acoustical fields in *Mhz*-range were generated and measured [11]. The helical acoustical wavefronts were recorded. Let us to obtain the exact expression for spatial distribution of the sound intensity near optical phase singularity in Brillouin medium using equation for acoustical field  $\mathbf{Q}_{twisted}$ . The expression for intensity of hypersound field  $I_{sound}$  reads immediately from the general expressions for electrostrictive nonlinearity [10, 19]:

$$\mathbf{I}_{sound} \approx |\mathbf{E}(z, r, \phi, t)|^2 = |E_{p,s}^o|^2 [1 + \cos[(\omega_p - \omega_s)t - (k_p + k_s)z + 2\ell\phi]] r^{2\ell} \exp\left[-\frac{2r^2}{D^2(1 + z^2/(k_p^2 D^4))}\right]. \quad (14)$$

We designated this acoustic vortex field as  $\mathbf{Q}_{twisted}$  having in mind helical distribution of intensity (fig. 4). It is clear that such vortex possesses *doubled* angular momentum, as it seen from doubled azimuthal angle  $2\ell\phi$  in self-similar argument of  $\cos$  in (14). In addition the complex acoustic envelope  $Q_{twisted}$  could be derived in steady-state regime due to the fact of the strong dumping of acoustical field. The lifetime for hypersound wave  $\Gamma^{-1}$  is of the order of the several nanoseconds for typical liquid and gaseous media[10]. Thus expression for acoustical envelope  $Q_{twisted}$  is obtained in steady-state from (3) using (9) :

$$Q_{twisted} \approx E_p E_s^* \approx \exp[+i2\ell\phi] r^{2\ell} \exp\left[-\frac{2r^2}{D^2(1 + z^2/(k_p^2 D^4))}\right]. \quad (15)$$

Evidently the envelope of acoustic wave  $Q_{twisted}$  has helical wavefront with doubled topological charge  $2\ell$ . The twisted spatiotemporal acoustic field  $\mathbf{Q}_{twisted}$  has the following form:

$$\mathbf{Q}_{twisted} \approx \mathbf{E}_p \mathbf{E}_s^* \approx \exp[i(\omega_p - \omega_s)t - i(k_p + k_s)z + i2\ell\phi] r^{2\ell} \exp\left[-\frac{2r^2}{D^2(1 + z^2/(k_p^2 D^4))}\right]. \quad (16)$$

The phase dislocation of acoustic wave rotates with acoustical frequency  $\Omega_a = \omega_p - \omega_s$ . The speed of translational motion in *Z* - *direction* of rotating turns of an acoustical spring is exactly equal to the speed of sound  $v_a$ . The rotating spring could be visualized by currently available experimental tools [11], because the transverse size of beam necklace could be easily changed e.g. by additional lenses.

The previous exact expressions (12, 14, 16) are based upon elementary exact solutions of the *parabolic* wave equations in the form of the first order **LG**. This simplification became possible due to geometrical separation of the **OA** with weak interaction of counter-propagating beams from **PCM** where strong interaction of the optical fields  $\mathbf{E}_p$  and  $\mathbf{E}_s$  takes place. The straightforward generalization is to be made taking into account the *elongated geometry* of phase singularities inside speckle pattern within SBS-mirror volume (fig. 2) [10]. The expression for the optical fields near the phase singularity with topological charge  $\ell$  could be generalized in the following form:

$$\mathbf{E}_{(p,s)}(z, r, \phi, t) = E_{p,s}^o r^\ell \exp[-i\omega_{(p,s)}t \pm ik_{(p,s)}z \pm i\ell\phi] f(r, z), \quad (17)$$

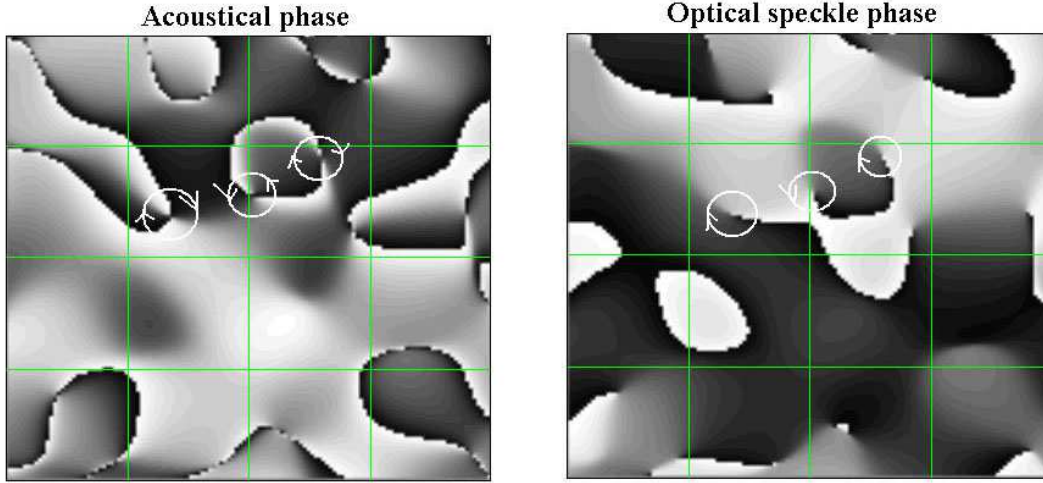


**Figure 5.** Comparison of acoustical (left) and optical *speckle* (right) fields inside Brillouin mirror pumped by multimode random phase field. The optical vortices on right panel are designated by white circles with one arrow. The phase is changed from 0 to  $\pm 2\pi$  in motion around *optical* phase singularity. The collocated acoustical vortices on the left panel are shown by white circles with two arrows. The phase is changed from 0 to  $\pm 4\pi$  in motion around *acoustical* phase singularity. The transverse  $X$ ,  $Y$  scale is  $100 \times 100 \mu\text{m}$ .

where  $f(r, z)$  - is a smooth function elongated in  $Z$ -direction. The inequality of the forward  $\mathbf{E}_p$  and backward  $\mathbf{E}_s$  fields amplitudes does not affect qualitatively the helical interference patterns (fig. 4) in the regime of weak saturation, because the Brillouin wavefront reversal mirrors with random phase plate have sufficiently high (approximately 0.9) phase-conjugating fidelity[16]:

$$K = \frac{|\int \mathbf{E}_p \mathbf{E}_s^* d\vec{r}|^2}{(\int |\mathbf{E}_p|^2 d\vec{r})(\int |\mathbf{E}_s|^2 d\vec{r})}, \quad (18)$$

The experimentally verified procedure utilizes the thin transparent glass plates with chaotic phase modulation (fig. 2) which have transverse correlation length of about tens of microns. Such geometry looks promising for realization of the phase-conjugation of **LG** and to overcoming a difficulties reported earlier [17]. Because of high degree of phase-conjugation fidelity of the forward  $\mathbf{E}_p$  and backward  $\mathbf{E}_s$  fields one may consider the transverse distributions of pump and Stokes fields near entrance window of **PCM** as almost identical. Thus the above expressions (12, 14, 16) for spring interference patterns might be valid for speckle fields as well. This enables us to plot transverse distributions of the optical and acoustical phases in output planes of **PC**-mirror and **OA** in a similar way, where phase-conjugated Stokes field  $\mathbf{E}_s$  is in a good correlation with the pump field  $\mathbf{E}_p$ . Choosing the  $8 \times 8$  random plane waves superposition for  $\mathbf{E}_p$  and  $\mathbf{E}_s \approx \mathbf{E}_p^*$  we obtained using (15) the transverse distributions of the phase of the envelope of optical speckle field  $\arg(E_p(\vec{r}_\perp))$  and for envelope of a field of collocated acoustical vortices  $\arg(Q_{twisted}(\vec{r}_\perp))$ . The acoustical vortices have doubled topological charges (fig. 5).

In summary we demonstrated that the wavefront - reversal mirrors are chiral optical antennas. The elementary consideration of conservation laws including conservation of **AM** shows the existence of twisted rotating structures inside an *ideal* phase-conjugator. For stimulated Brillouin scattering mirror the rotating spiral interference pattern modulates the dielectric permittivity  $\epsilon$  via electrostriction. The dynamical equations give the exact expressions for sound intensity inside acoustical phase singularity which is *collocated* with optical phase singularity. It is worth to mention the model presented above does not take into account the several essential features of Brillouin **PCM**, e.g. longitudinal dependence of optical fields and corresponding spatial mismatch of their amplitudes. The reflection of the both elementary optical vortices like **LG** and speckle fields as well is accompanied by excitation inside SBS wavefront-reversal mirror of *sonic* vortices with doubled topological charge. Internal helical waves and spiral modulation of dielectric permittivity induce local anisotropy inside the phase-conjugating mirror and forces the exchange of angular momentum. The new experimental geometry is proposed (fig. 2) in order to observe parametric excitation of an isolated acoustical vortices inside **OA**. Interference pattern near each phase singularity in a speckle pattern rotates clockwise with angular speed  $\Omega = \omega_p - \omega_s$  regardless to the sign of spirality of the interference spring. The rotation changes direction to counter-clockwise for all singularities in a speckle for anti-Stokes frequency of retroreflected wave. The angular speed  $\Omega$  depends also on the physical mechanism of wavefront reversal. It could span from units of *Hz* for the photorefractive crystals to *terahertz* range for Raman phase-conjugators[10].

The connection of the angular momenta of the incident and reflected photons seems to be valid for any other nonlinear **PCM** including photorefractive one. In order to transfer **OAM** the rotating intensity springs should excite the helical waves intrinsic to given type of phase conjugating mirror. The peculiarities of photorefractive media, e.g. nonstationary vortex reflection, screening, vortex splitting and "disappearance of nonlinearity" [22] also deserves special attention. The successful wavefront reversal of complex images obtained else the first experiments with photorefractive phase conjugators [23] is an indirect evidence for existence of internal helical waves in the volume of photorefractive **PCM** and other phase-conjugators alike liquid-crystal light valves.

The correspondence between formulas for classical fields  $\mathbf{E}_p$ ,  $\mathbf{E}_s$  and  $\mathbf{Q}$  and quantum field description by means of Heisenberg's secondary-quantization  $\hat{\Psi}$  - operators [1] will be given elsewhere. Briefly in quantum picture of ideal phase conjugator (fig.1) each incident photon with orbital angular momentum  $L_z = \ell\hbar$  decays to reflected photon with opposite  $L_z = -\ell\hbar$  projection on propagation axis and a quantum of internal wave with doubled **OAM**  $L_z^a = 2\ell\hbar$ .

## References

- [1] E.M.Lifshitz, L.P.Pitaevskii, and V.B.Berestetskii 1982 "*Quantum Electrodynamics*"

(Landau and Lifshitz Course of Theoretical Physics, Butterworth-Heinemann, Oxford)  
Vol.4 Ch.I § 6,8.

- [2] L.Allen, M.W.Beijersbergen, R.J.C.Spreeuw and J.P.Woerdman 1992 Phys.Rev. A **45** 8185-8189.
- [3] J.F.Nye and M.V.Berry 1974 Proc. R. Soc. London, Ser.**A336** 165.
- [4] M.S.Soskin and M.V.Vasnetsov 2001 "Progress in Optics" ed. E.Wolf ( Amsterdam:Elsevier) **42** 219-276.
- [5] J.Leach,M.J.Padgett,S.M.Barnett,S.Franke-Arnold, and J.Courtial 2002 Phys. Rev. Lett. **88** 257901.
- [6] V.S.Liberman and B.Ya.Zeldovich 1992 Phys.Rev. A **46** 5199.
- [7] J.D.Jackson 1962 "*Classical Electrodynamics*" (New York:Wiley ).
- [8] L.A.Weinstein 1969 "*Open resonators and open waveguides*". (Colorado:Golem Press).
- [9] R.A. Beth 1936 Phys.Rev. **50** 115.
- [10] B.Y.Zeldovich, N.F.Pilipetsky and V.V.Shkunov 1985 "Principles of Phase Conjugation" (Berlin:Springer-Verlag ).
- [11] J-L.Thomas and R.Marchiano 2003 Phys. Rev. Lett. **91** 244302.
- [12] D.V.Petrov and J.W.R.Tabosa 1999 Phys. Rev. Lett. **83** 4967.
- [13] K.-P.Marzlin,W.Zhang, and E.M.Wright 1997 Phys.Rev.Lett. **79** 1997.
- [14] P.N.Lebedev 1901 Annalen der Physik **6** 433.
- [15] M.J.Friese,J.Euger,H.Rubinstein-Dunlop 1996 Phys.Rev. A **54** 1543.
- [16] N.G.Basov, I.G.Zubarev, A.B.Mironov, S.I.Mikhailov and A.Y.Okulov 1980 JETP, **52** 847.
- [17] F.A.Starikov, Yu.V.Dolgopolo, A.V.Kopalkin, G.G.Kochemasov, S.M.Kulikov and S.A.Sukharev 2006 J. Phys. IV France **133** 683-685 .
- [18] V. G. Veselago 1968 Sov. Phys. Usp. **10** 509.
- [19] R.W.Boyd,K.Rzazewsky,P.Narum 1990 Phys.Rev. A **42** 5514.
- [20] A.Yu.Okulov 2008 J.Mod.Opt. **55** n.2 241-257.
- [21] V.N.Tsyтовich 2007 Phys.Usp. **177** n.4 428.
- [22] A.V.Mamaev,J.Saffmam and A.A.Zozulya 1996 Phys.Rev. A **56** R1713.
- [23] J.Feinberg and R.W.Hellwarth 1981 Opt.Lett. **6** 257.